



Fabrication of Polyethersulfone Membrane with Manganese Ferrite/Graphite Nanohybrid for Dye Filtration

Yekti Purnama Utami¹, Yap Wing Fen², Eny Latifah¹, ST. Ulfawanti Intan Subadra¹, Ahmad Taufiq^{1,*}

Received
8 July 2023

Revised
12 September 2023

Accepted for Publication
30 September 2023

Published
31 October 2023

¹ Departement of Physics, Faculty of Mathematic and Natural Science, Universitas Negeri malang, Jl. Semarang No 5, Malang, 65145, Indonesia.

² Department of Physics, Faculty of Science, Universiti Putra Malaysia 43400 UPM Serdang Selangor, Malaysia

*Corresponding Author's E-mail: ahmad.taufiq.fmipa@um.ac.id



This work is licensed under a Creative Commons Attribution-ShareAlike 4.0 International License

Abstract

Membrane technology has received significant attention in wastewater treatment. In this study, membranes were fabricated by the phase-inversion method from manganese ferrite/graphite nanohybrids embedded in a polyether sulfone membrane matrix. Manganese ferrite is synthesized from natural materials of iron sand with Mn using the co-precipitation method, which is then combined with 3-Aminoopropyl trimethoxy silane (APTES), while graphite is obtained from coconut shells. The membrane shows good performance, with a pure water flux value of 170.01 Lm-2h. The membrane also showed good methylene blue filtration capability with a flux value of 130.74 Lm-2h and a color difference from methylene blue.

Keywords: Manganese Ferrite, Graphite, Filtration Membrane, Methylene Blue

1. Introduction

Currently, membrane technology has received much attention in the fields of wastewater treatment, desalination, and drinking water treatment [1], [2] because it has high efficiency [2], [3], low energy consumption [4], low cost, good performance, and ease of use [1], [5]. Generally, polymer membranes are more widely used because of their good physical and chemical properties [6] and are available at low prices [1]. One of the polymers that is often used is polyether sulfone (PES) because it has good chemical and thermal stability [7], and good membrane formation capabilities [1], [7]. However, the hydrophobicity of PES can affect membrane performance, such as high color and salt rejection [6], low chemical resistance, and poor membrane fouling [8].

There are several ways to reduce and prevent membrane fouling, one of which is by modifying the membrane using hydrophilic nanoparticles [1], [2], [6]. Membrane modification with hydrophilic components can increase hydrophilicity and permeability, as well as control membrane flux [1], [2]. Apart from that, the addition of hydrophilic nanoparticles can also increase the membrane's adsorption ability against dyes and heavy metals [3]. Some commonly used nanoparticles are Ag, TiO₂, SiO₂ [5], Al₂O₃, ZnO, and Fe₃O₄ [6]. Among these nanoparticles, Fe₃O₄ has attracted a lot of attention because it has been proven to be able to adsorb heavy metals and dyes in water [9]. Fe₃O₄ is also able to remove catalysts and toxic elements from industrial waste [8]. However, the low surface charge of Fe₃O₄ can cause aggregation and reduce membrane efficiency [6]. The addition of a higher concentration of Fe₃O₄ in the membrane can also cause damage to the membrane structure, in the form of increasing pore size and increasing membrane roughness [7].

Several studies have proposed ways to improve membrane structure, including nanohybrid [6] and doping Fe₃O₄ with other materials [10]. A nanohybrid is a combination of two different nanoparticles that leverages the special properties of both. In this research, graphite is used for the Fe₃O₄ nanohybrid. Graphite is a natural layered inorganic material with abundant resources and easy to

produce at low cost. Graphite has excellent electrical conductivity, low density, strong environmental adaptability, and high temperature resistance [11]. Fe₃O₄/graphite can increase surface area via open pores. In addition, the strong magnetic dipole interaction between Fe₃O₄ nanoparticles and graphite can create high chemical stability [12].

Doping Fe₃O₄ with various transition metals can provide significant changes in increasing the activation ability of H₂O₂ and electronic properties, so as to improve the adsorption performance of the material [13], [14]. The magnetic spinel that is widely used is ferrite (MFe₂O₄; M= Ni, Zn, Co, Mn, Cu, Cr, or Mg) [14], [15]. In this research, Mn is used because Mn has a relatively the same atomic radius to Fe, apart from that, Mn has characteristics like Fe in the form of ferromagnetic properties [16]. The addition of Mn can also increase UV absorbance in Methylene Blue degradation [17].

In addition, the filtration membrane performance was improved by modifying the manganese ferrite with APTES. The silica groups in the APTES structure can react with the hydroxyl groups of manganese ferrite. Then, manganese ferrite is functionalized by NH₂ groups on the surface. Another APTES structure reacts with carboxylic acids and hydroxyl groups on the graphite surface [6]. In this research, membrane fabrication will be carried out using the phase-inversion method with PES and manganese ferrite/graphite nanohybrid. manganese ferrite nanoparticles were synthesized from iron sand, and graphite nanoparticles were synthesized from coconut shells.

2. Methods

1.1. Materials

Graphite powder from coconut shell, iron sand, sodium nitrate (NaNO₃), sulfuric acid (H₂SO₄), potassium permanganate (KMnO₄), hydrogen peroxide (HO), and distilled water. Hydrochloric Acid (HCl) 12 M Merck, Ammonium Solution (NH₄OH) Merck, MnCl₂·4H₂O, Dimethylformamide (DMF) Merck, N, N-dimethylacetamide (DMAc) Merck, ethanol Merck, and PES sigma.

1.2. Synthesis of Manganese Ferrite/Graphite Nanohybrid

Synthesis of the manganese ferrite/Graphite Nanohybrid begins with the synthesis of manganese ferrite nanoparticles using the co-precipitation method. A total of 20 grams of iron sand was reacted with 58 ml of HCl, as in our previous research [18]. The second stage is making graphite from coconut shells using the hummer method. A total of 5 grams of graphite and 5 grams of NaNO₃ were dissolved in 120 ml of H₂SO₄ in an ice bath for 30 minutes. Then, KMnO₄ was slowly added and stirred for 30 minutes at a temperature of 20°C. Then, continued stirring for 3 hours at room temperature, followed by titration of 150 ml of distilled water at 95 °C and stirring for 3 hours. After that, 50 ml of hydrogen peroxide was added slowly. The solution was washed with 1M HCl and ethanol until neutral pH, then dried at 60°C for 6 hours.

The third stage is the preparation of the manganese ferrite/Graphite nanohybrid. Before that the manganese ferrite nanoparticles are modified first using APTES. The manganese ferrite and APTES were dissolved in 200 ml of ethanol for 30 minutes, then the solution was slowly added to 40 ml of distilled water and stirred at 78 °C. The resulting precipitate was washed several times with distilled water and dried for 2 hours at 60 °C to obtain f-manganese ferrite nanoparticles. Preparation of the f-manganese ferrite nanohybrid and graphite began by dispersing 1 g of graphite in DMF using an ultrasonic bath for 30 minutes, then adding f-manganese ferrite and sonicating for 30 minutes. Next, the solution was stirred for 4 hours at 105°C. The resulting precipitate was washed with ethanol then dried.

1.3. Fabrication of manganese ferrite/graphite/PES

The filtration membrane was fabricated using the phase-inversion method, in which 1 g of PES was dissolved in N, N-dimethylacetamide (DMAc). Then, the manganese ferrite/graphite nanohybrid nanoparticle powder was added and sonicated for 30 minutes until a black solution was formed. Once the mixture is homogeneous, it is printed onto a glass plate. The membrane was soaked in a coagulation bath containing distilled water for 24 hours.

2. Results and Discussion

The diffraction pattern of manganese ferrite/GO nanoparticles is shown in Figure 1. The sample shows diffraction patterns corresponding to the hkl planes (2 2 0), (3 1 1), (4 0 0), (4 2 2), (5 1 1), and

(4 4 0). This is in accordance with the diffraction pattern of the Fe_3O_4 sample. The sharp and strong diffraction peak around $2\theta = 26.5^\circ$ (0 0 2) confirms the presence of graphite material [12]. The characteristic peak shift indicates the interaction between manganese ferrite and graphite in forming the manganese ferrite/graphite nanohybrid [5], [19].

The manganese ferrite/graphite nanohybrid was characterized by FTIR, as shown in Figure 2. There is a peak at 3615 cm^{-1} , which corresponds to the O-H group. The peaks at 2931 cm^{-1} and 2805 cm^{-1} indicate the functional group of C-H. The C=O group in carboxylic acids is shown at 1737 cm^{-1} . The peaks at 1106 cm^{-1} and 1040 cm^{-1} are attributed to Si-O-Si stretching, indicating the presence of APTES in the nanohybrid. The transmittance peaks at 687 cm^{-1} and 555 cm^{-1} correspond to magnetite-stretching Mn-O and Fe-O vibrations. When manganese and iron ions are evenly distributed in the spinel crystal lattice, there is a shift in the absorption peaks of the characteristic vibrations [20].

The hysteresis curve of manganese ferrite/graphite nanohybrid is shown in Figure 3. Based on the figure, the manganese ferrite/graphite nanohybrid exhibits superparamagnetic properties as evidenced by an S-shaped hysteresis curve with remanent magnetization (M_r) and coercivity (H_c) values close to zero. The saturation magnetization of manganese ferrite/Graphite nanohybrid is 3.86 emu/g . The saturation magnetization properties of materials are directly proportional to the particle size, where increasing particle size causes an increase in saturation magnetization [21] because the domain walls of large particles are easier to rotate [18].

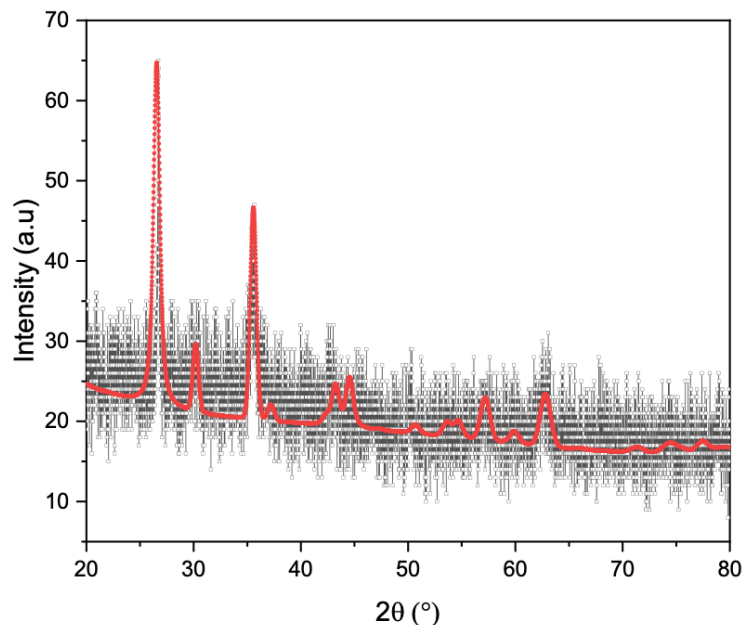


Figure 1. XRD Results for Manganese Ferrite/Graphite Nanohybrid.

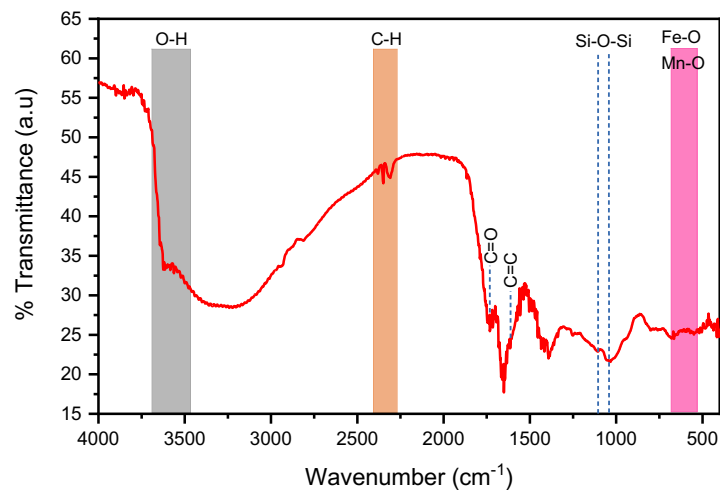


Figure 2. FTIR Results for Manganese Ferrite/Graphite Nanohybrid.

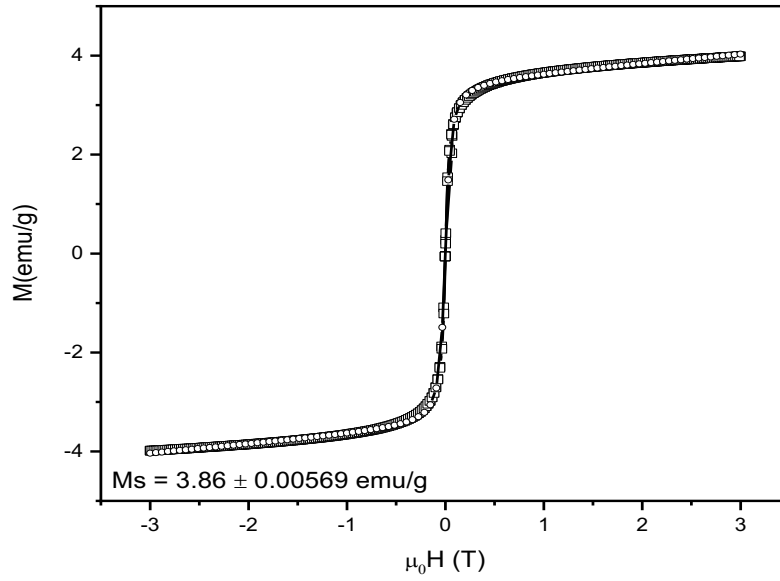


Figure 3. VSM Test Results for Manganese Ferrite/Graphite Nanohybrid.

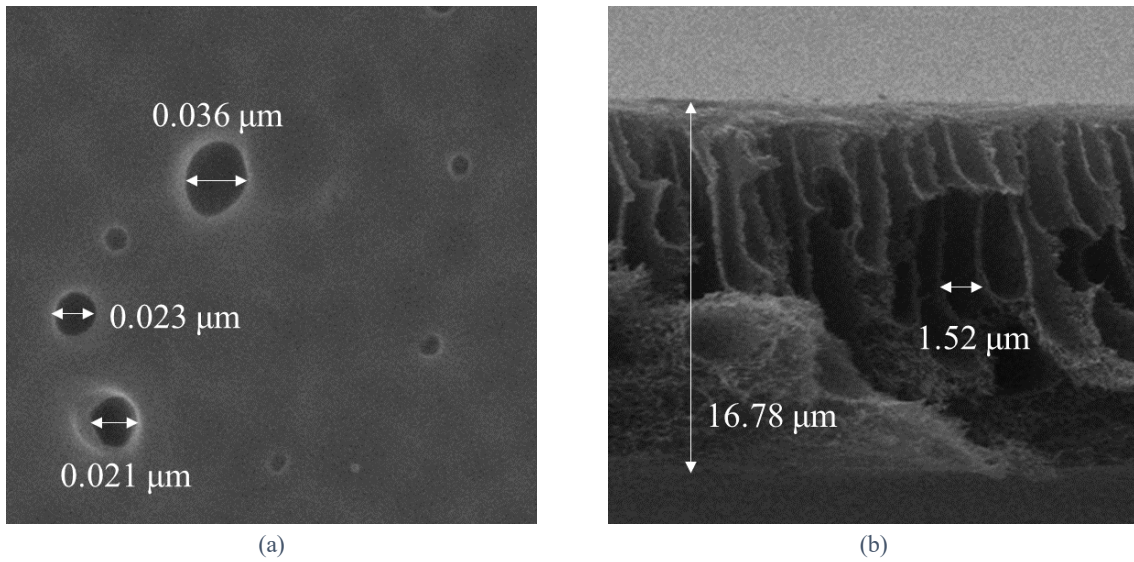


Figure 4. SEM Images of Membrane Viewed from (a) Top and (B) Cross-Section.



Figure 5. Result of Methylene Blue Filtration.

The membrane was characterized by SEM to determine its surface and transverse structures. Figure 4 is the result of the SEM membrane test. Figure 4(a) shows that the pore size distribution is not uniform, with an average pore size of 0.026 μm . Figure 4 (b) shows that the membrane has a thickness of 16.78 μm . Apart from that, there is an asymmetrical structure of the membrane in the form of a selectively dense upper skin layer, and a thick porous sub-layer with finger-like pores called macro void cavities [2], [6] nanohybrids in the membrane solution where during the coagulation process there is a mass transfer between the solvent (DMAc) and non-solvent (water) phase [6], [22]. Macro void cavities and membrane thickness can influence the value of water flux, causing the membrane to have more water molecule permeation paths so that water flux increases.

Membrane performance tests include pure water flux and the methylene blue rejection test. The pure water flux can be calculated from the amount of water that passes through the membrane with a surface area of 9 cm^2 , tested using distilled water and 50 ppm methylene blue at 1 bar every 5 minutes for 15 minutes. The pure water flux was 170.01 Lm^{-2}h for pure water and 130.74 Lm^{-2}h for the methylene blue solution. The difference in the flux values of pure water and methylene blue is caused by differences in the concentration of the solution that passes through the membrane. The greater the solution concentration, the lower the flux is because particles in the solution cannot pass through the membrane, causing fouling. The results of the methylene blue filtration test are shown in Figure 5. It can be seen that the filtered methylene blue has a brighter color than before filtering.

3. Conclusion

The filtration membrane was successfully fabricated using a nanohybrid of manganese ferrite/graphite and polyethersulfone (PES). The membrane has pores with a diameter of 0.026 μm . The membrane performance showed good results, with fluxes of pure water and methylene blue of 170.01 Lm^{-2}h and 130.74 Lm^{-2}h , respectively.

Acknowledgment

This work was financially supported by DRTPM Kemendikbudrsitek through PPS PTM scheme for AT with Grant No. 3.4.133/UN32.20.1/LT/2023.

References

- [1] C. P. Vun, A. W. Mohammad, T. Y. Haan, and E. Mahmoudi, "Evaluation of Iron oxide decorated on graphene oxide ($\text{Fe}_3\text{O}_4/\text{GO}$) nanohybrid incorporated in PSF membrane at different molar ratios for Congo red rejection," *J Teknol*, vol. 79, no. 1–2, pp. 73–81, 2017, doi: 10.11113/jt.v79.10440.
- [2] Y. Huang, C. fa Xiao, Q. lin Huang, H. liang Liu, J. qiang Hao, and L. Song, "Magnetic field induced orderly arrangement of $\text{Fe}_3\text{O}_4/\text{GO}$ composite particles for preparation of $\text{Fe}_3\text{O}_4/\text{GO}/\text{PVDF}$ membrane," *J Memb Sci*, vol. 548, pp. 184–193, Feb. 2018, doi: 10.1016/j.memsci.2017.11.027.
- [3] S. Jahankhah, M. M. Sabzehmeidani, M. Ghaedi, K. Dashtian, and H. Abbasi-Asl, "Fabrication polyvinyl chloride mixed matrix membrane via embedding $\text{Fe}_3\text{O}_4/\text{polydopamine}/\text{Ag}$ nanocomposite for water treatment," *Mater Sci Eng B Solid State Mater Adv Technol*, vol. 285, Nov. 2022, doi: 10.1016/j.mseb.2022.115935.
- [4] L. Dong, M. Li, S. Zhang, X. Si, Y. Bai, and C. Zhang, " $\text{NH}_2\text{-Fe}_3\text{O}_4$ -regulated graphene oxide membranes with well-defined laminar nanochannels for desalination of dye solutions," *Desalination*, vol. 476, no. October 2019, p. 114227, 2020, doi: 10.1016/j.desal.2019.114227.
- [5] P. V. Chai, J. Y. Law, E. Mahmoudi, and A. W. Mohammad, "Development of iron oxide decorated graphene oxide ($\text{Fe}_3\text{O}_4/\text{GO}$) PSf mixed-matrix membrane for enhanced antifouling behavior," *Journal of Water Process Engineering*, vol. 38, Dec. 2020, doi: 10.1016/j.jwpe.2020.101673.
- [6] M. Mirzaei, T. Mohammadi, N. Kasiri, and M. A. Tofighy, "Fabrication of magnetic field induced mixed matrix membranes containing $\text{GO}/\text{Fe}_3\text{O}_4$ nanohybrids with enhanced antifouling properties for wastewater treatment applications," *J Environ Chem Eng*, vol. 9, no. 4, Aug. 2021, doi: 10.1016/j.jece.2021.105675.

- [7] J. Alam, L. A. Dass, M. Ghasemi, and M. Alhoshan, "Synthesis and optimization of PES-Fe₃O₄ mixed matrix nanocomposite membrane: Application studies in water purification," *Polym Compos*, vol. 34, no. 11, pp. 1870–1877, Nov. 2013, doi: 10.1002/pc.22593.
- [8] Munasir and R. P. Kusumawati, "Synthesis and Characterization of Fe₃O₄@rGO Composite with Wet-Mixing (ex-situ) Process," *J Phys Conf Ser*, vol. 1171, no. 1, pp. 1–6, 2019, doi: 10.1088/1742-6596/1171/1/012048.
- [9] N. Munasir, R. P. Kusumawati, D. H. Kusumawati, Z. A. I. Supardi, A. Taufiq, and Darminto, "Characterization of Fe₃O₄/rGO composites from natural sources: Application for dyes color degradation in aqueous solution," *International Journal of Engineering, Transactions A: Basics*, vol. 33, no. 1, pp. 18–27, 2020, doi: 10.5829/ije.2020.33.01a.03.
- [10] Z. Qi, T. P. Joshi, R. Liu, H. Liu, and J. Qu, "Synthesis of Ce(III)-doped Fe₃O₄ magnetic particles for efficient removal of antimony from aqueous solution," *J Hazard Mater*, vol. 329, pp. 193–204, 2017, doi: 10.1016/j.jhazmat.2017.01.007.
- [11] K. Deng *et al.*, "The resin-ceramic-based Fe₃O₄/graphite composites rapidly fabricated by selective laser sintering for integration of structural-bearing and broadband electromagnetic wave absorption," *J Alloys Compd*, vol. 943, May 2023, doi: 10.1016/j.jallcom.2023.169120.
- [12] R. Atchudan, T. N. J. Immanuel Edison, S. Perumal, R. Vinodh, N. Muthuchamy, and Y. R. Lee, "One-pot synthesis of Fe₃O₄@graphite sheets as electrocatalyst for water electrolysis," *Fuel*, vol. 277, Oct. 2020, doi: 10.1016/j.fuel.2020.118235.
- [13] Y. Pu, X. Tao, X. Zeng, Y. Le, and J. F. Chen, "Synthesis of Co-Cu-Zn doped Fe₃O₄ nanoparticles with tunable morphology and magnetic properties," *J Magn Magn Mater*, vol. 322, no. 14, pp. 1985–1990, Jul. 2010, doi: 10.1016/j.jmmm.2010.01.018.
- [14] Y. Zhang *et al.*, "Spinel MnFe₂O₄ nanoparticles (MFO-NPs) for CO₂ cyclic decomposition prepared from ferromanganese ores," *Ceram Int*, vol. 46, no. 9, pp. 14206–14216, Jun. 2020, doi: 10.1016/j.ceramint.2020.02.229.
- [15] M. Y. Nassar and M. Khatib, "Cobalt ferrite nanoparticles: Via a template-free hydrothermal route as an efficient nano-adsorbent for potential textile dye removal," *RSC Adv*, vol. 6, no. 83, pp. 79688–79705, 2016, doi: 10.1039/c6ra12852a.
- [16] E. Ekasari, "Aplikasi Nanopartikel Magnetik Didoping Dengan Mn Untuk Adsorpsi Logam Berat Dalam Air Sungai Siak."
- [17] A. Wahab *et al.*, "Dye degradation property of cobalt and manganese doped iron oxide nanoparticles," *Applied Nanoscience (Switzerland)*, vol. 9, no. 8, pp. 1823–1832, Nov. 2019, doi: 10.1007/s13204-019-00970-1.
- [18] A. Taufiq *et al.*, "Studies on Nanostructure and Magnetic Behaviors of Mn-Doped Black Iron Oxide Magnetic Fluids Synthesized from Iron Sand," *Nano*, vol. 12, no. 9, Sep. 2017, doi: 10.1142/S1793292017501107.
- [19] P. V. Chai, E. Mahmoudi, Y. H. Teow, and A. W. Mohammad, "Preparation of novel polysulfone-Fe₃O₄/GO mixed-matrix membrane for humic acid rejection," *Journal of Water Process Engineering*, vol. 15, pp. 83–88, Feb. 2017, doi: 10.1016/j.jwpe.2016.06.001.
- [20] A. S. Korsakova, D. A. Kotsikau, Y. S. Haiduk, and V. V. Pankov, "Synthesis and physicochemical properties of Mn_xFe_{3-x}O₄ solid solutions," *Kondensirovannye Sredy Mezhfaznye Granitsy*, vol. 22, no. 4, pp. 466–472, Dec. 2020, doi: 10.17308/kcmf.2020.22/3076.
- [21] S. Tabatabai Yazdi, P. Iranmanesh, S. Saeednia, and M. Mehran, "Structural, optical and magnetic properties of Mn_xFe_{3-x}O₄ nanoferrites synthesized by a simple capping agent-free coprecipitation route," *Mater Sci Eng B Solid State Mater Adv Technol*, vol. 245, pp. 55–62, Jun. 2019, doi: 10.1016/j.mseb.2019.05.009.
- [22] S. Kamari and A. Shahbazi, "Biocompatible Fe₃O₄@SiO₂-NH₂ nanocomposite as a green nanofiller embedded in PES-nanofiltration membrane matrix for salts, heavy metal ion and dye removal: Long-term operation and reusability tests," *Chemosphere*, vol. 243, Mar. 2020, doi: 10.1016/j.chemosphere.2019.125282.
- [23] V. M. Alfianti and M. Munasir, "Fabrication and Characterization of GO-Fe₃O₄/PSF Membrane with Phase Inversion Method," *JPSE (Journal of Physical Science and Engineering)*, vol. 6, no. 2, pp. 55–60, Jul. 2021, doi: 10.17977/um024v6i22021p055.